

IFMIF-DONES HFTM neutronics modeling and nuclear response analyses

Yuefeng Qiu*, Frederik Arbeiter, Ulrich Fischer, Florian Schwab

Karlsruhe Institute of Technology, Hermann-von-Helmholtz-Platz 1, D-76344 Eggenstein-Leopoldshafen, Germany



ARTICLE INFO

Keywords:
IFMIF-DONES
HFTM
Neutronics
DPA
gas production

ABSTRACT

IFMIF-DONES (International Fusion Materials Irradiation Facility- DEMO Oriented NEutron Source) is a neutron irradiation facility aiming at providing material irradiation data for the construction of DEMOnstration fusion power plants. This work presents nuclear analyses and associated neutronics modeling conducted on an updated design of the High Flux Test Module (HFTM) of IFMIF-DONES. Neutron fluxes, damage dose rates and gradients, gas production and nuclear heating have been calculated for the standard profile in $20 \times 5 \text{ cm}^2$ and a reduced size in $10 \times 5 \text{ cm}^2$ of the deuteron beam with 40 MeV energy and 125 mA current. The results indicate that the reduced beam can provide higher damage dose rates fulfilling the DONES requirement. On the other hand, the reduced beam size results in less irradiation uniformity, higher gas production to damage dose ratios, as well as stronger peak nuclear heating.

1. Introduction

IFMIF-DONES (International Fusion Materials Irradiation Facility- DEMO Oriented NEutron Source) [1,2] is a IFMIF-based neutron irradiation facility which aims at providing the irradiation data required for the construction of a DEMOnstration fusion power plant (DEMO). DONES consists of only one of the IFMIF accelerators (40 MeV and 125 mA), and utilizes only the High Flux Test Module (HFTM) for the irradiation of material specimens. The HFTM is the key component to provide the material irradiation data which fulfill the mission of DONES.

The damage dose (quantified in terms of Displacements Per Atom, DPA) for which the DEMO first wall (FW) will be designed is 20 dpa (based on the NRT damage model [3]) in the initial phase and 50 dpa in the second phase [4]. As top level requirements, the DONES HFTM aims at providing a 0.3 l irradiation volume with 20–30 dpa in <2.5 years, and 0.1 l volume with 50 dpa in <3 years [5]. Recently, the HFTM design was updated to provide more irradiation volume based on the fact that the HFTM is the only test module in DONES. A new set of nuclear response analyses has to be consequently carried out to qualify the HFTM against the requirements. Also as an option, the deuteron beam can be concentrated from a standard beam profile size of $20 \times 5 \text{ cm}^2$ to a reduced size of $10 \times 5 \text{ cm}^2$ to produce higher damage rates on the center specimen capsules. The irradiation performances of using these two beam sizes were not fully analyzed so far. For this reason, the modeling and nuclear responses analyses of the updated HFTM have been carried out and are presented in this paper.

2. HFTM neutronics modeling

The DONES HFTM design is shown in Fig. 1. The outer shape is similar to the HFTM design in IFMIF/EVEDA phase [6], but the major changes are the container and the capsule design. In the IFMIF/EVEDA phase, the HFTM-V design has a vertical layout with 8 compartments and 3 irradiation rigs in each compartment. The DONES HFTM container has still 8 compartments, whereas each compartment is subdivided into 4 slots, and the container thickness (in beam direction) is increased from 55.0 mm to 102.2 mm, i.e. almost doubled. The “rig” design of the IFMIF/EVEDA HFTM has been replaced with direct-inserted capsules. Also stiffening plates are added between the capsules to increase the structure stability. The center 4 columns of capsules serve as irradiation volume, while the other 4 columns provide the function of lateral neutron reflectors due to low DPA. The specimen stack in the capsule has dimensions of 16.0 mm in thickness (x-direction), 40.0 mm in width (y-direction), and 81.0 mm in height (z-direction). The material samples are arranged inside the specimen stack, immersed in liquid metal to improve the temperature uniformity. The temperature is controlled through the electric heater wires brazed into the capsules. The IFMIF/EVEDA concept of using NaK-78 eutectic liquid metal has been replaced by liquid sodium due to the production of a notable amount of Argon gas inside the capsule.

The HFTM body is made of X2CrNiMo17-12-2(N) (or, SS316L(N)) stainless steel, which is comply with the RCC-MRx code [7]. The maximum amount of impurities given in the RCC-MRx code are considered, providing the Co, Nb and Ta contents of 500 ppm, 100 ppm and

* Corresponding author.

E-mail address: yuefeng.qiu@kit.edu (Y. Qiu).

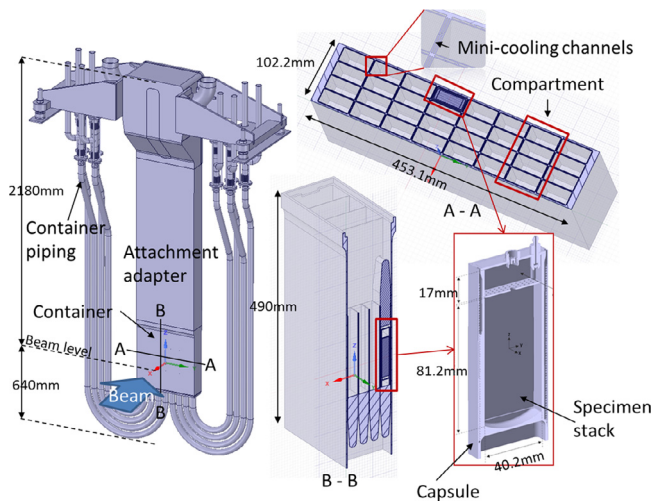
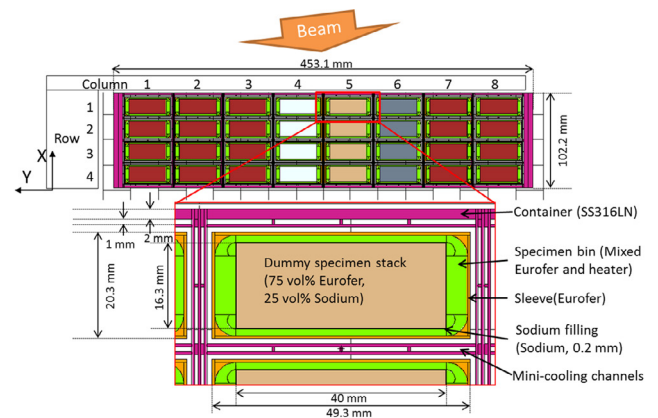
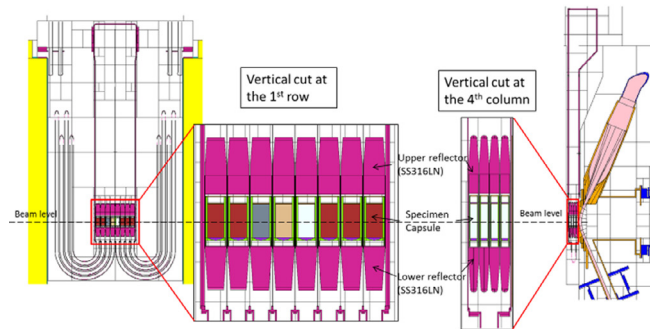


Fig. 1. CAD model of the DONES HFTM.



(a) Horizontal cut-view at the beam level



(b) Vertical cut-view the 1st row and the 4th column

Fig. 2. MCNP plots of the HFTM model (2D cuts).

100 ppm. It is noted that the ^{60}Co is one of the most important radionuclides contributing to the dose of the HFTM after 10~100 years cooling. However, under the hard neutron spectrum in the HFTM, the amount of ^{60}Co produced from the activation of natural Co (100% abundance of ^{59}Co) is small, thus the Co impurity is not of significance to the HFTM activation. The specimen capsule is made of 73.3 vol% Eurofer-97 and the rest of heater material. The dummy specimen stack is a mixture with 75 vol% of Eurofer-97 and 25 vol% of natural sodium. Based on the chemical composition given in [8], the impurities of Co, Nb and Ta contents in Eurofer-97 is 100 ppm, 50 ppm and 1500 ppm, respectively, which provides conservative values for the activation analyses.

Simplifications have been made mainly for the CAD geometry of the specimen capsules, as well as other small unnecessary details, e.g. fillets and chamfers. However, the mini-cooling channels are preserved. The simplified HFTM model has been converted into neutronics model for the Monte Carlo code MCNP6 [9], using the McCad software [10]. Plots of the MCNP model of the HFTM are shown in Fig. 2. This MCNP model has been integrated into the DONES test cell (TC) model [11], replacing the IFMIF/EVEDA HFTM. This new TC neutronics model (denoted as version “mdl8.2.0”), which also includes the TC surrounding rooms and an update of the target assembly with a bayonet back-plate [12], has been adopted as the current reference model. This model has been subsequently tested and validated for its geometry correctness.

3. Nuclear response analyses

The McDeLicious code [13], which is an extension of the MCNP Monte Carlo code with the capability to simulate the deuterium-lithium neutron source on the basis of evaluated $d + ^6\text{Li}$ cross section data [14], was employed for the neutronics calculations. This code has been recently upgraded to the latest MCNP version 6.1.0. This upgraded version, denoted “McDeLicious-17”, has been tested and confirmed to generate identical source particle data as the previous version McDeLicious-11. The neutron cross-section library FENDL-3.1b [15] has been adopted for the neutron transport calculations.

The reference deuteron beam profile in the IFMIF/EVEDA phase was used, which has a footprint on a $20 \times 5 \text{ cm}^2$ area. For the reduced beam size of $10 \times 5 \text{ cm}^2$, the same beam profile and beam power (40 MeV and 125 mA) were used but the horizontal dimension is scaled by a factor of 0.5. The results calculated for these two beam sizes are compared in this paper. If no special indication is given, the cut-views in the following figures are plot either on the horizontal X-Y plane at the beam level, or on the vertical X-Z plane crossing the target center. The mesh tallies used have a common resolution of $5 \times 5 \times 5 \text{ mm}^3$

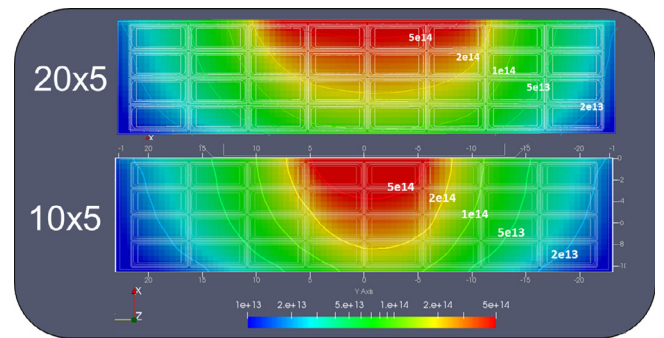


Fig. 3. Neutron flux ($\text{n}/\text{cm}^2/\text{s}$) distribution on the horizontal cut-plane.

covering the specimen capsule and reflector. The distribution maps in the figures are overlaid to a sketch of the actual HFTM geometry.

3.1. Neutron flux

The neutron flux map of the HFTM is shown in Fig. 3. The typical neutron flux range in the center four compartment of HFTM is $1 - 5 \times 10^{14} \text{ n}/\text{cm}^2/\text{s}$. The flux distribution in the HFTM is asymmetric, since the deuteron beam incident angle of 9° of IFMIF is kept in DONES. This is to enable a future upgrade to the full IFMIF with two accelerators and avoid the direct back-scattering of neutrons to the beam line. This asymmetry might affect thermal and mechanical analyses (e.g. increasing simulation region), as well as in-site irradiation characterizations since the DPA in each capsule might differ. The peak flux under the reduced beam size is clearly higher than that under standard beam size, but the difference becomes less significant at the lateral side. The neutron flux spectra, averaged over the center 4 column of the

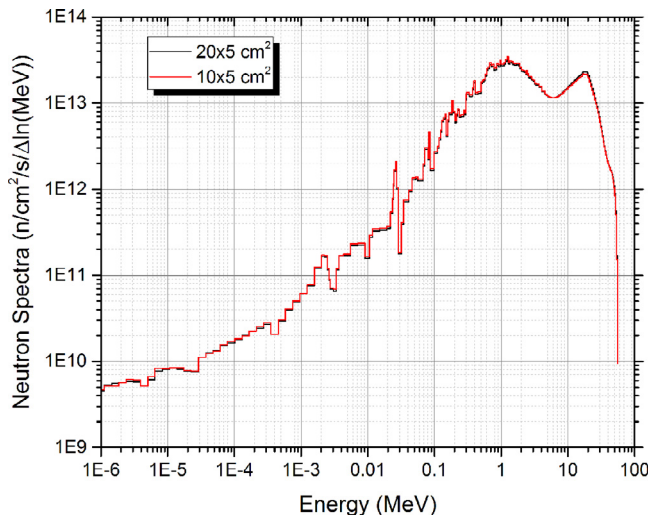


Fig. 4. Neutron flux spectra averaged over the whole HFTM specimen region.

HFTM specimen region, are shown in Fig. 4. It shows that the spectra produced at both beam sizes are quite similar.

3.2. Damage dose

The DPA performance of the HFTM is essential in fulfilling the DONES requirement. Fig. 5 shows the map of the DPA rate in dpa per full power year (dpa/fpy) calculated from the neutron flux mesh tally, provided with the McDeLicious calculation, and multiplied with the DPA cross-section of natural iron. Therefore, it gives the iron equivalent DPA value based on the NRT damage model [3]. As one can see from this figure, the damage rate of the two center capsules of the 1st row is up to 20 dpa/fpy at standard beam size, and increases up to 30 dpa/fpy at the reduced beam size. Therefore, higher damage rates in a relative smaller volume can be achieved with a reduced beam size. The exact volume provided in the specimen stack which corresponds to a specified damage rate is calculated using a well-configured mesh tally. This mesh tally has mesh intervals coinciding with the boundaries of the specimen stacks so that the mesh cell inside the stacks can be extracted and analyzed. The results are shown in Fig. 6 in a way that the volume which has DPA rate larger than the specified DPA value is plotted as a function of DPA. The “Spec. region” indicates the volume evaluated on the center four compartments, while the “Spec. stack” indicates the volume in the specimen stacks. As reference, the DPA requirements of DONES mentioned in Section 1 can be translated into the first requirement (R-1): 8–12 dpa/fpy in a 0.3 l volume; and the second requirement (R-2): 16.7 dpa/fpy in a 0.1 l volume. In the case of using standard beam size, the volume for R-1 is ~0.27 l, and for R-2 it is <0.06 l, which is only more than a half of R-2. For the reduced beam size, a similar volume (0.27 l) is provided for R-1, while the volume

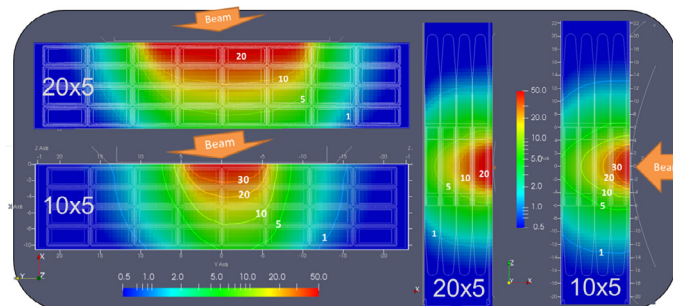


Fig. 5. DPA rate (dpa/fpy) distribution on the horizontal cut-plane (left) and the vertical cut-plane (right).

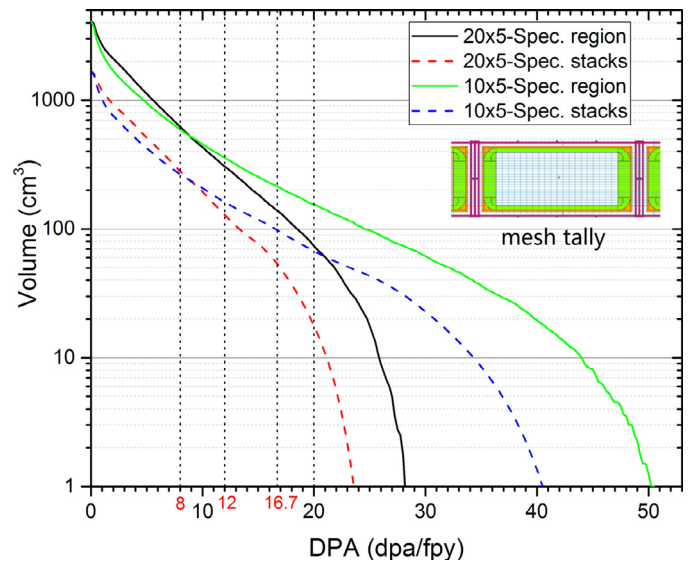


Fig. 6. Plot of volume-DPA curves. “Spec. region” covers the center 4 compartments, and the “Spec. stack” considers only the volume in specimen stacks.

available for R-2 increases to 0.10 l, thus meeting very well the DONES requirement. Therefore, using the reduced beam size can accelerate the material irradiation in DONES and fulfill its requirements.

Apart from the DPA rate, the uniformity of the irradiation is also important for characterizing the material. As another top level requirement, the DPA gradient in the high flux region has to be <10% over a gauge volume [5]. The gauge volume of a specimen has a typical dimension of 2–3 mm, thus the gradient should be in principle less than 25%/cm. The damage gradient is shown in Fig. 7. Since the gradient on the neutron forward direction (X direction) will be much larger, the specimens are mostly arranged on the Y-Z plane [6]. Therefore, the gradients are calculated on the Y-Z plane giving the worst gradient of a mesh cell to 9 neighboring cells. The gradient is normalized to the DPA value in order to obtain a relative gradient value (unit: %/cm). From Fig. 7 it is clear that the gradient requirement is better met with the standard beam size. It is noted that, when using the reduced beam size, only the center two (instead of four) compartments are considered for the material irradiation. Table 1 shows the evaluation of volume fraction of the center compartments in different gradient ranges. The standard beam size produces better gradient conditions compared to the reduced beam size for about 10%. It provides a useful hint that the horizontal beam size of 10 cm can be slightly increased in order to provide better gradient conditions for the center two compartments.

3.3. Gas production

The gas production has a synergistic effect with the DPA. It directly impacts the diffusion of damage defects. The gas-DPA ratio, i.e. the

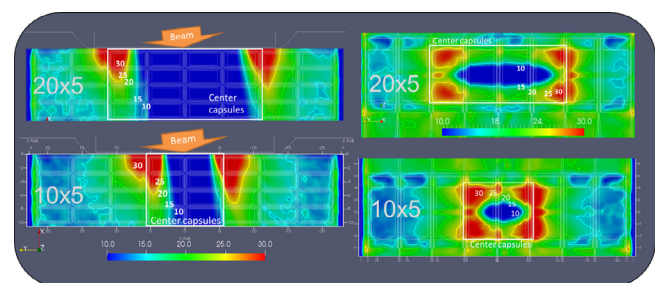
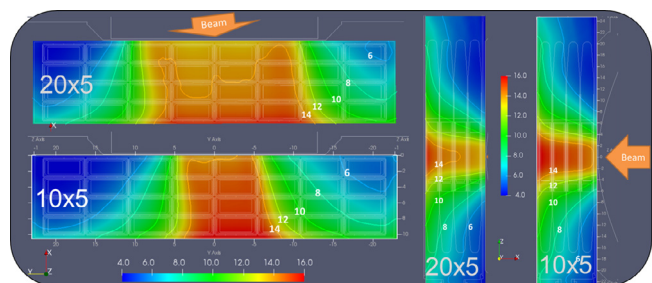


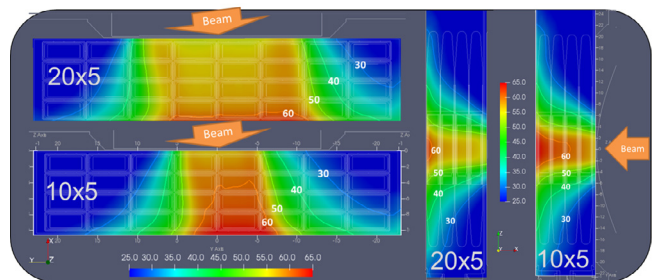
Fig. 7. Relative DPA gradient calculated on the Y-Z plane. Left: horizontal cut-view at the beam level; Right: vertical cut-view at center of the 1st row.

Table 1
Volume fraction in the center compartments with DPA gradient in different ranges.

Gradient (%/cm)	20 × 5 (1963.5 cm ³)	10 × 5 (981.7 cm ³)
<15	33%	21%
15–25	45%	46%
25–50	22%	33%



(a) He-ratio (He-appm/dpa)



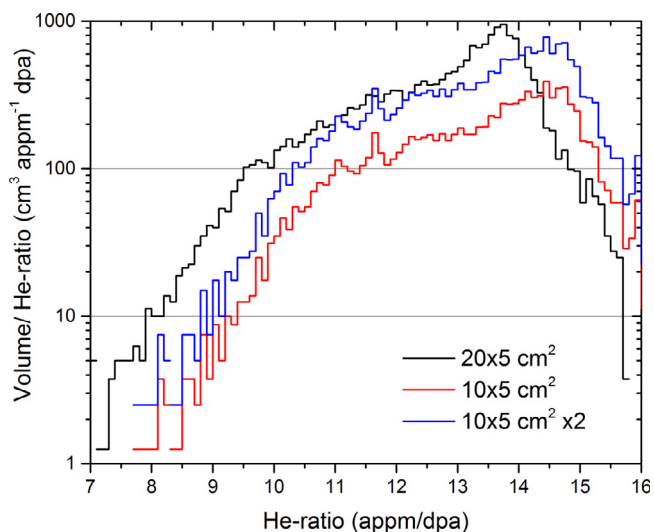
(b) H-ratio (H-appm/dpa)

Fig. 8. Gas-DPA ratios on the horizontal cut-plane (left) and the vertical cut-plane (right).

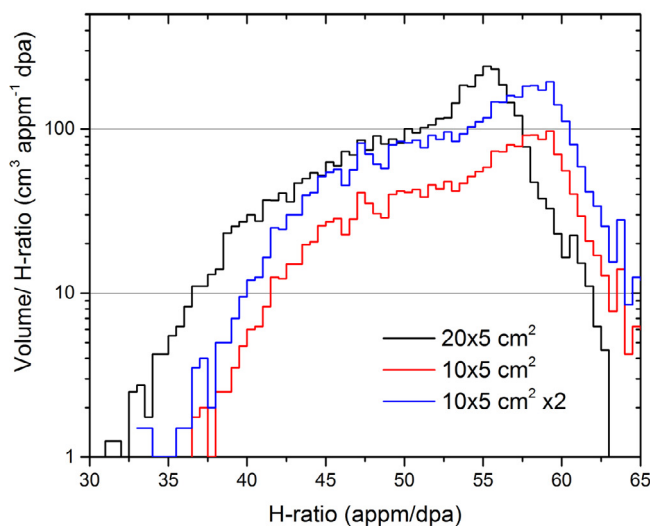
helium production to DPA ratio (or He-ratio, unit: He-appm/dpa) and the hydrogen production to DPA ratio (or H-ratio, unit: H-appm/dpa) are shown in Fig. 8. The gas productions are calculated on a superimposed mesh tally assuming full of Eurofer-97. It is noted that for the FW in DEMO, the He- and H-ratios expected for steels are at 11–12 He-appm/dpa and 45–55 H-appm/dpa, which is estimated based on the 1.8 GW fusion power concept with HCPB blanket [4,16]. As seen from Fig. 8, the values for the 1st row of the center compartments are 12 - 14 He-appm/dpa and 50 - 60 H-appm/dpa, which slightly deviate from typical DEMO conditions. However, when compared to other available neutron sources [17], these values fit much better to the acceptable range. With a reduced beam size, the gas-DPA ratios are increased overall. Detailed comparisons are presented using for the volumes as a function of gas-DPA ratios as shown in Fig. 9. In addition, the results for the center two compartments with reduced beam size are multiplied by the factor 2 in this figure to allow a better comparison with the results for the center four compartments with the regular beam size. It is clear that the curves for the reduced beam size are shifted to the higher energy range which increase ~ 1 He-appm/dpa and ~ 4 H-appm/dpa, or ~ 7% in general.

3.4. Nuclear heating

The nuclear heating distributions in the HFTM are shown in Fig. 10. They are calculated using a mesh tally by averaging the nuclear heating of mixed materials in each mesh cell. The neutron and gamma heating contributions are summed up. The peak heating value is up to 17 W/cm³ at standard beam size, while it increases up to 28 W/cm³ with the reduced beam size. Therefore, using the reduced beam size imposes



(a) He-ratio



(b) H-ratio

Fig. 9. Irradiation volumes as a function of gas-DPA ratios. The volume is normalized by $\Delta(\text{gas-DPA ratio})$. The results of the reduced beam size on the center two compartments are doubled for the comparison to the standard beam size on the center four compartments.

higher requirements on the HFTM design in handling the more pronounced heating distributions and maintaining the structural integrity.

It is noted that the peak heating might be underestimated due to the drawback of the calculation method: a void fraction inside a mesh cell will reduce the heat density. To avoid this, superimposed mesh tallies with each one assuming full of one material, e.g. Eurofer, SS316L(N), are used for scoring the actual heating without void fraction. The heating data on the specific components were interpolated from these meshes, using some multi-physics coupling tools McMeshTran [18], and provided for the HFTM thermal and structural analyses.

4. Conclusions and discussions

Nuclear analyses and associated neutronics modeling have been conducted on the updated design of the DONES HFTM. The neutronics model of the HFTM has been converted from the CAD geometry, and integrated into the neutronics model of the DONES TC. Neutron fluxes,

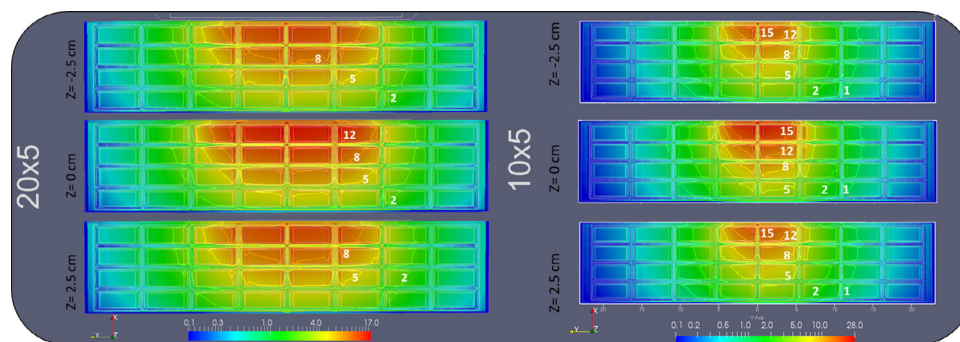


Fig. 10. Nuclear heating (W/cm^3) distribution in the HFTM.

DPA rates and gradients, the gas production, and the nuclear heating have been calculated using two deuteron beam profile size: $20 \times 5 \text{ cm}^2$ (standard size) and $10 \times 5 \text{ cm}^2$ (reduced size).

Considering the DONES requirements, the reduced beam size show a better performance in providing higher damage rates on the required irradiation volume. For the required volume with 20–30 dpa in <2.5 years, the reduced beam size provides a similar volume (0.27 liter) as the standard beam size; for the required volume with 50 dpa in <3 years, the reduced beam size provides the volume (0.10 liter) as required, while the standard beam size provides <0.06 liter. On the other hand, the reduced beam size leads to less preferable damage gradients for about 10%. The gas productions to DPA ratios in the HFTM are slightly higher than for DEMO first wall condition. The use of a reduced beam size increases the gas-DPA ratio for $\sim 7\%$, and also increases the peak heating which might bring more challenges for the HFTM design.

Acknowledgments

This work has been carried out within the framework of the EUROfusion Consortium and has received funding from the Euratom research and training programme 2014–2018 under grant agreement No 633053. The views and opinions expressed herein do not necessarily reflect those of the European Commission.

References

- [1] J. Knaster, The accomplishment of the engineering design activities of IFMIF/EVEDA: the European–Japanese project towards a Li(d,xn) fusion relevant neutron source, *Nucl. Fusion* 55 (8) (2015) 086003.
- [2] A. Ibarra, et al., A stepped approach IFMIF/EVEDA towards IFMIF, *Fusion Sci. Technol.* 66 (2014) 252–259.
- [3] M.T. Robinson, Basic physics of radiation damage production, *J. Nucl. Mater.* 216 (1994) 1–28 [https://doi.org/10.1016/0022-3115\(94\)90003-5](https://doi.org/10.1016/0022-3115(94)90003-5).
- [4] D. Stork, P. Agostini, J.-L. Boutard, et al., Materials R&D for a timely DEMO: key findings and recommendations of the EU Roadmap Materials Assessment Group, *Fusion Eng. Des.* 89 (2014) 1586–1594.
- [5] A. Ibarra, R. Román, DONES Conceptual Design Report, (2014).
- [6] F. Arbeiter, A. Abou-Sena, J. Averhals, et al., Design description and validation results for the IFMIF high flux test module as outcome of the EVEDA phase, *Nucl. Mater. Energy* 9 (2016) 59–65.
- [7] AFCEN, Design and Construction Rules for Mechanical Components of Nuclear Installations (RCC-MRx), ISBN: 2-913638-57-6, Edition with first Addendum 2013, (2012) AFCEN no 132–2012.
- [8] R. Lindau, A. Möslang, M. Rieth, Present development status of EUROFER and ODS-EUROFER for application in blanket concepts, *Fusion Eng. Des.* 75–79 (2005) 989–996.
- [9] J.T. Goorley, M.R. James, T.E. Booth, et al., Initial MCNP6 Release Overview-MCNP6 Version 1.0, Los Alamos National Laboratory (LANL), 2013.
- [10] L. Lu, Y. Qiu, U. Fischer, Improved solid decomposition algorithms for the CAD-to-MC conversion tool McCad, *Fusion Eng. Des.* 124 (2017) 1269–1272 <https://doi.org/10.1016/j.fusengdes.2017.02.040>.
- [11] K. Tian, B. Ahedo, F. Arbeiter, Overview of the current status of IFMIF-DONES test cell biological shielding design, *Proceeding of 13th International Symposium on Fusion Nuclear Technology*, Kyoto, Japan, 2017 Sept 25–29.
- [12] G. Micciché, A. Aiello, D. Bernardi, The European contribution to the development and validation activities for the design of IFMIF lithium facility, *Fusion Eng. Des.* 88 (2013) 791–795.
- [13] S.P. Simakov, U. Fischer, K. Kondo, P. Pereslvtsev, Status of the McDeLicious approach for the D-Li neutron source term modeling in IFMIF neutronics calculations, *Fusion Sci. Technol.* 62 (2012) 233–239.
- [14] A. Konobeyev, Yu. Korovin, P. Pereslvtsev, U. Fischer, U. Von Möllendorff, Development of methods for calculation of deuteron-lithium and neutron-lithium cross sections for energies up to 50 MeV, *Nucl. Sci. Eng.* 139 (2001) 1–23.
- [15] The Fusion Evaluated Nuclear Data Library, FENDL-3.1b, <http://www.nds.iaea.org/fendl/>.
- [16] M.R. Gilbert, S.L. Dudarev, S. Zheng, L.W. Packer, J.C. Sublet, An integrated model for materials in a fusion power plant: transmutation, gas production, and helium embrittlement under neutron irradiation, *Nucl. Fusion* 52 (2012) 083019 <https://doi.org/10.1088/0029-5515/52/8/083019>.
- [17] N. Baluc, K. Abe, J.L. Boutard, et al., Status of R&D activities on materials for fusion power reactors, *Nucl. Fusion* 47 (2007), <https://doi.org/10.1088/0029-5515/47/10/S18>.
- [18] Y. Qiu, P. Lu, U. Fischer, P. Pereslvtsev, S. Kecskes, A generic data translation scheme for the coupling of high-fidelity fusion neutronics and CFD calculations, *Fusion Eng. Des.* 89 (2014) 1330–1335 <https://doi.org/10.1016/j.fusengdes.2014.02.044>.